HHS Public Access

Author manuscript

J Trauma Acute Care Surg. Author manuscript; available in PMC 2023 March 01.

Published in final edited form as:

J Trauma Acute Care Surg. 2022 March 01; 92(3): 489–498. doi:10.1097/TA.0000000000003487.

Mesenchymal Stem Cell Extracellular Vesicles Mitigate Vascular Permeability and Injury in the Small Intestine and Lung in a Mouse Model of Hemorrhagic Shock and Trauma

Mark Barry, MD[1], **Alpa Trivedi, PhD**[2], **Praneeti Pathipati, PhD**[2], **Byron Y. Miyazawa, BS**[2], **Lindsay R. Vivona, BS**[2], **Padma Priya Togarrati, PhD**[3], **Manisha Khakoo**[2], **Heather Tanner, MS**[3], **Philip Norris, MD**[3], **Shibani Pati, MD, PhD**[2,*]

[1]University of California, San Francisco. Department of Surgery. 513 Parnassus Ave. San Francisco, CA 94143

[2]University of California, San Francisco. Department of Laboratory Medicine. 513 Parnassus Ave. San Francisco, CA 94143

[3]Vitalant Research Institute. 270 Masonic Ave. San Francisco, CA 94118

Abstract

Background: Hemorrhagic shock and trauma (HS/T)-induced gut injury may play a critical role in the development of multi-organ failure. Novel therapies that target gut injury and vascular permeability early after HS/T could have substantial impacts on trauma patients. In this study we investigate the therapeutic potential of human mesenchymal stem cells (MSCs) and MSC-derived extracellular vesicles (MSC EVs) *in vivo* in HS/T in mice and *in vitro* in Caco-2 human intestinal epithelial cells.

Methods: *In vivo*, using a mouse model of HS/T, vascular permeability to a 10kD dextran dye and histopathologic injury in the small intestine and lungs were measured among mice. Groups were 1) sham, 2) HS/T+lactated Ringer's (LR), 3) HS/T+MSCs, and 4) HS/T+MSC EVs. *In vitro*, Caco-2 cell monolayer integrity was evaluated by an epithelial cell impedance assay. Caco-2 cells were pre-treated with control media, MSC conditioned media (CM), or MSC EVs, then challenged with hydrogen peroxide (H_2O_2).

Results: *In vivo*, both MSCs and MSC EVs significantly reduced vascular permeability in the small intestine (fluorescence units: Sham 456±88, LR 1067±295, MSC 765±258, MSC EV 715±200) and lung (Sham 297±155, LR 791±331, MSC 331±172, MSC EV 303±88). Histopathologic injury in the small intestine and lung was also attenuated by MSCs and MSC

*Indicates corresponding author to whom correspondence should be addressed: Shibani Pati, MD PhD, Professor, Department of Laboratory Medicine, 513 Parnassus Avenue, San Francisco, CA 94143, Shibani.Pati@ucsf.edu, Phone: (713)299-0788.

Author Contributions: All authors participated in manuscript preparation. S.P. participated in the planning, execution, and analysis of the experiments. M.B., A.T., and P.P. planned the experiments. M.B., P.P., B.M., and L.V. performed the *in vitro* assays. P.P.T, H.N., and P.N. performed flow cytometry and interpretation. M.B. and P.P. performed the *in vivo* experiments. M.K. and M.B. performed the histological analysis. M.B. performed statistical analyses. M.B and A.T. prepared the figures and interpreted the data.

Conflicts of Interest: The authors have no conflicts of interests to disclose.

Presentation: This research is being presented at the 80th Annual Meeting of the American Association for the Surgery of Trauma and Clinical Congress of Acute Care Surgery; October 2, 2021; Atlanta, GA.

EVs. *In vitro*, MSC CM but not MSC EVs attenuated the increased permeability among Caco-2 cell monolayers challenged with H_2O_2.

Conclusion: MSC EVs recapitulate the effects of MSCs in reducing vascular permeability and injury in the small intestine and lungs *in vivo*, suggesting MSC EVs may be a potential cell-free therapy targeting multi-organ dysfunction in HS/T. This is the first study to demonstrate MSC EVs improve both gut and lung injury in an animal model of HS/T.

Level of evidence: N/A (Basic Science)

Keywords

Hemorrhagic shock; Mesenchymal stem cells; Extracellular vesicles; Vascular permeability; Gut and Lung Injury

BACKGROUND

Among critically injured patients surviving their initial traumatic insult, multiple organ dysfunction syndrome (MODS) remains an important determinant of long-lasting morbidity and mortality.(1–3) The development of acute respiratory distress syndrome (ARDS) is a particularly serious sequela occurring in approximately 14% of severely injured trauma patients and carrying an estimated mortality rate of 22% that has remained unchanged for several decades.(4, 5) The pathophysiology of ARDS and MODS may be attributed in part to the endotheliopathy of trauma (EOT), a triad composed of vascular barrier compromise, systemic inflammation, and aberrant clotting that occurs early after injury.(6, 7) Early damage to the gut barrier after hemorrhagic shock and trauma (HS/T) has also been shown to play an integral role in the development of lung injury and MODS.(8, 9) While the development of modern trauma systems and damage control resuscitation have led to significant improvements in the care of the injured patient,(10, 11) therapies that effectively target early gut injury and mitigate the EOT and MODS after trauma are lacking.

Cellular therapies for trauma and critical care applications are a novel approach that may hold great potential for targeting the EOT and gut and lung injury in trauma patients.(12) Mesenchymal stem cells (MSCs) derived from bone marrow are known to have anti-inflammatory, antimicrobial, and anti-apoptotic properties.(13, 14) MSCs have been demonstrated in preclinical studies to play a therapeutic role in a variety of disease states characterized by inflammation and vascular dysfunction, including ARDS, traumatic brain injury (TBI), and sepsis.(12, 14) Our lab has previously shown that MSCs have the capacity to attenuate lung injury in a rodent model of HS/T.(15) MSCs also decrease epithelial barrier permeability and histologic injury in the intestine in animal models of both intestinal ischemia-reperfusion and colitis.(16–19)

Many of the therapeutic effects of MSCs are mediated through the secretion of soluble factors and extracellular vesicles (EVs), rather than engraftment and differentiation into other cell types.(13, 20) EVs are membrane-enclosed nanoparticles released from cells and contain RNA, DNA, lipids, and protein from the cell of origin. EVs play an important role in cell-to-cell communication by transferring their cargo to recipient cells, and by doing so MSC EVs have demonstrated therapeutic effects on immunomodulation and wound

healing.(20) Delivery of MSC EVs has thus been proposed as a novel “cell-free” therapy that may be able to recapitulate the benefits of MSCs without many of the logistical and practical challenges presented by standard cell therapies.(21) In rodent models, MSC EVs indeed replicate the therapeutic effects of MSCs in their ability to attenuate lung vascular permeability after HS/T,(22) decrease lung inflammation in bacterial pneumonia,(23) and protect against lung injury induced by intestinal ischemia-reperfusion.(24) Whether MSCs and MSC EVs are protective against injury to the gut specifically in a model of HS/T has not been studied.

In this study, we investigate the effects of MSCs and MSC EVs both *in vivo* in an established mouse model of HS/T *and in vitro* on Caco-2 intestinal epithelial cell monolayer integrity.(25–27) We hypothesize that both MSCs and MSC EVs will be protective against vascular permeability and injury in both the small intestine and lung in mice subjected to HS/T and will mitigate injury-induced permeability of a Caco-2 cell monolayer.

METHODS

MSC Cell Culture

Human bone marrow-derived MSCs passage 1 were obtained from Rooster Bio Inc. (Frederick, MD). MSCs were expanded initially on the Terumo Quantum device (Terumo, Lakewood, CO) to generate passage 2 cells that were used in all studies. MSCs were grown in Mesenchymal Stem Cell Growth Medium 2 (PromoCell, Heidelberg, Germany) and were maintained at 37°C and 5% CO_2 in a humidified incubator.

Isolation of MSC EVs

MSCs were grown to 80% confluence and then serum-starved for 48 hours. The conditioned media was then collected and centrifuged at 1500g × 10 minutes to remove cells and debris then filtered using a 0.22μm filter. EVs were isolated from the conditioned media using the Labscale Tangential Flow Filtration System with the Pellicon® XL50 Cassette with Biomax® 500 kDa Membrane (MilliporeSigma, Burlington, MA). Aliquots of isolated EVs in phosphate buffered saline (PBS) were stored at −80°C.

Characterization of MSCs and EVs

The size and particle concentration of the isolated MSC EVs were determined by nanoparticle tracking analysis using the NanoSight NS300 (Malvern Panalytical, Westborough, MA). Samples were diluted 1:10 in particle-free PBS and the data were analyzed using NTA 3.2 Dev Build 3.2.16 (Malvern Panalytical). Protein content was quantified using a DeNovix DS-11 Spectrophotometer (DeNovix, Wilmington, DE).

For phenotypic characterization, flow cytometric analysis of the MSC EVs was conducted using EV-specific tetraspanin markers CD9, CD63, and CD81, MSC markers CD73, CD90, and CD105, and negative control markers HLA-DR, CD45, and CD31 (Biolegend, San Diego, CA). Relative particle size was determined using 0.2, 0.5, 2.0, and 3.0μm Flow Cytometry Sub-micron Particle Size reference beads (Thermo Scientific, Waltham, MA). EV samples were also lysed using 10% Nonident P-40 (NP-40 (New England Biolabs, Inc.,

Ipswich, MA) and re-run to exclude false positive background as described previously.(22) Samples were run on an LSR II benchtop flow cytometer (BD Biosciences, San Jose, CA) and data were analyzed using FlowJo software (Tree Sar, Inc., Ashland, OR).

Animals

The animal studies were performed with approval of the Institutional Animal Care and Use Committee (IACUC) at UCSF. The experiments were conducted in compliance with the ARRIVE guidelines for animal models and National Institutes of Health (NIH) guidelines on the use of laboratory animals. All mice were housed in a room with access to food and water ad libitum, controlled temperature and 12:12-hour light-dark cycles. Mice were acclimatized in the housing facility for a minimum of three days prior to study intervention.

Hemorrhagic Shock and Trauma (HS/T) Mouse Model

Male C57BL6 mice, 8–12 weeks old, were obtained from The Jackson Laboratory (Sacramento, CA) (N=35 total). Under inhaled isoflurane anesthesia, animals were placed on a heating plank to maintain body temperature between 35°C and 37°C. Femoral arterial catheters were flushed with heparin and then cannulated into the femoral arteries of both legs. No additional heparin was used. The right catheter was used for continuous blood pressure monitoring (PowerLab 8, AD Instruments, Dunedin, New Zealand), and the left catheter was used for blood withdrawal and resuscitation. A 2cm midline laparotomy was performed to induce additional trauma, and internal organs were inspected. Mice were then bled to a mean arterial blood pressure (MAP) of 35 mmHg for 90 minutes.(22, 25) After the 90-minute shock period, mice received a 200μL fluid treatment containing 1) lactated Ringer's (LR) (N=10), 2) 1×10^6 MSCs in LR (N=9), or 3) MSC EVs (30μg protein) in PBS (N=8). These doses were chosen based on previous work in our lab demonstrating efficacy of MSCs and EVs in attenuating pulmonary vascular permeability in this model(22) and fall within the range of EV dosing used in other rodent models.(23, 28, 29) Sham mice underwent cannulation without laparotomy or blood withdrawal (N=6). Mice were monitored hemodynamically for an additional 30 minutes after resuscitation and were then allowed to ambulate freely for 60 minutes. All mice were run sequentially and were assigned to groups as test interventions were ready to be administered. No mice were excluded from analysis.

MSC EV Labeling and Tracking After HS/T

Labeled MSC EVs were administered to one naïve mouse and one mouse that underwent HS/T as described above to track their location after delivery. For MSC EV labeling, 3μL of CellVue Claret Far Red lipophilic dye (Sigma Aldrich, St. Louis, MO) was added to 120μg of MSC EVs in a total volume of 2mL (using Diluent C) for 10 minutes at room temperature. Labeled MSC EVs were then precipitated out using ExoQuick (660μL, SBI Biosciences, Palo Alto, CA) incubation overnight at 4°C followed by a 3000g spin for 15 minutes. MSC EVs were resuspended in 0.1μM filtered PBS. Half of the labeled EVs were administered via retro-orbital injection to the naïve mouse and the other half via the femoral artery to the HS/T mouse. 30 minutes after injection, a segment of small intestine and the left lung were harvested and flash frozen in isopentane, then sectioned on a Leica CM 1950 Cryostat (Leica Biosystems, Wetzlar, Germany) at 10μm thickness. Sections were imaged

with a Nikon Eclipse 80i microscope (Nikon, Melville, NY) with RT-scmos camera (SPOT Imaging, Sterling Heights, MI).

In Vivo Vascular Permeability in the Small Intestine and Lung

Three hours after the initiation of shock, mice were anesthetized with isoflurane and 0.2mL of 0.2mg/mL 10 kDa dextran conjugated with Alexa Fluor 680 was administered via the femoral cannula as previously reported.(25, 30) Thirty minutes after injection, the mice were perfused with 30mL of ice-cold PBS via the left ventricle to flush the blood from the organs. The left lung and a 1cm segment of small intestine (9cm from the ileocecal valve) were harvested and scanned on the Odyssey CLx Imager (LI-COR, Lincoln, NE), and the infrared signal was read at 700nm to detect dye that had extravasated out of the vasculature into the tissue. Using Image Studio Version 5.2 (LI-COR), an average fluorescence intensity per area was quantitated for the lung and small intestine.

Histologic Analysis of the Small Intestine and Lung

The left lung and a 1cm segment of small intestine (7cm from the ileocecal valve) were post-fixed overnight in 4% paraformaldehyde at 4°C and dehydrated in 30% sucrose at 4°C for 3–5 days. The organs were embedded in Optimal cutting temperature (OCT) compound and stored at −80°C until they were sectioned on a Leica CM 1950 Cryostat (Leica Biosystems) at 10μm thickness. Tissue sections were stained with Hematoxylin & Eosin at the Mouse Pathology Core (University of California, San Francisco). Sections were imaged with a Revolve microscope (Echo Inc., San Diego, CA).

Scoring of Histologic Lung and Small Intestine Injury

Three lung sections per mouse were assessed and representative images were chosen. Three or more 100x magnification fields per mouse were evaluated by a blinded researcher using a scoring system from 1–4 to quantify inflammatory infiltration. A score of 1 is the least injured with less than 20% of the pulmonary area demonstrating inflammatory cell infiltration. A score of 2 indicates 20–40% inflammatory cell infiltration, 3 indicates 40–70% inflammatory cell infiltration, and 4 indicates 70–100% inflammatory cell infiltration. Wall thickening was assessed by the number of images with demonstrable alveolar wall thickening.(25)

Six small intestine sections per mouse were assessed and representative images were chosen. Four or more 100x magnification fields per mouse were evaluated by a blinded researcher and scored according to the Chiu grading system for intestinal ischemic mucosal lesions: 0, normal mucosa; 1, subepithelial bleb at tip of villus; 2, extension of the subepithelial space (upper half of villus; 3, massive epithelial lifting down the sides of villi; 4, frequent denuded villi; 5, loss of villous tissue and disintegration of the lamina propria.(31)

Caco-2 Cell Culture

Caco-2 human intestinal epithelial cells were obtained from American Type Culture Collection (ATCC, Manassas, VA). Caco-2 cells were grown in Eagle's Minimum Essential Medium (ATCC) supplemented with 20% Fetal Bovine Serum and 1% penicillin/streptomycin. Cells were maintained at 37°C and 5% CO_2 in a humidified incubator.

In Vitro Intestinal Epithelial Permeability Assay

Caco-2 cells (25,000 cells per well) were seeded onto a 96-well plate containing electrodes in each well pre-treated with L-cysteine. Cells were grown to form a confluent monolayer over 3 days. The integrity of the Caco-2 monolayer was measured using an electric cell-substrate impedance sensing system (ECIS 1600, Applied BioPhysics, Troy, NY). The cells were serum-starved and once resistances had stabilized were treated with MSC control media (25% volume concentration), MSC conditioned media (25% volume concentration), or MSC EVs (30μg protein/ml). MSC conditioned media contains the MSC secretome, whereas MSC control media is the growth media that has not been exposed to MSCs and thus does not contain any MSC secreted factors. Thirty minutes later the cell monolayers were challenged with 2.5mM hydrogen peroxide (H_2O_2) to induce oxidative stress and paracellular permeability. Impedance of the monolayer was analyzed at 1/4/32 kHz in 3-minute intervals. Data were normalized to the mean impedance of the cell monolayers before the treatments.

Statistical Analysis

Sample sizes were chosen based on previous work in our lab showing that 6–10 mice per group were needed to find statistical differences in vascular permeability and histologic injury.(22, 25) Data in this manuscript are presented as mean ± standard deviation. Means between groups were compared using one-way ANOVA with Tukey's post hoc tests. Mean arterial pressures were compared using repeated measures two-way ANOVA followed by Tukey's multiple comparison test. $P<0.05$ was considered significant. All analyses were performed using Prism 9.0 (GraphPad Inc., San Diego, CA).

RESULTS

Characterization of MSC EVs

The isolated MSC EVs used for this study were quantified using NanoSight, demonstrating a concentration of 1.16×10^9 particles/mL with a size peak at 123nm (Figure 1). This size is consistent with small EVs, which are secreted lipid membrane enclosed nanoparticles with sizes of less than 200nm.(32) The protein content of the isolated MSC EVs was 160μg/mL. To definitively characterize the MSC EVs, flow cytometry was used with markers specific to EVs (CD69, CD81, and CD9) and MSCs (CD73, CD105, and CD90) as well as negative controls (CD31, CD45, and HLA-DR). Of the EV markers and MSC markers tested, all were positive except for CD105, and the negative markers were indeed negative (Figure 1). Of note, others have also noted variability in CD105 expression among MSCs related to culture technique.(33, 34) Taken together these results indicate that the EV isolates tested and characterized were indeed MSC EVs.

MSC EVs traffic to the liver, spleen, kidney, lung, and ischemic hindlimb muscle after administration

MSC EVs labeled with a lipophilic dye were administered to one naïve mouse and one mouse after HS/T. Thirty minutes after delivery, in both the naïve and HS/T mouse, MSC EVs were detected predominantly in histologic sections of the liver and spleen but also

in the lung and kidney (Figure 2). Additionally, MSC EVs were detected in the hindlimb muscle only in the mouse subjected to HS/T, which notably involves instrumentation and ligation of the femoral artery and thus some degree of muscle ischemia. Labeled EVs were not detected in the blood or the small intestine 30 minutes after delivery.

MSCs and MSC EVs decrease intestinal and pulmonary vascular permeability in mice subjected to HS/T

Among mice subjected to HS/T and treated with LR, MSCs, or MSC EVs, MAPs during the 30-minute period after resuscitation were similar between groups (Figure 3A). The average fluorescence intensity of extravasated dye in the harvested small intestine and lung was measured at three hours after initiation of HS/T (Figure 3B, 3C). In the small intestine, HS/T resulted in increased vascular permeability in LR-treated mice compared to sham mice (sham 456±88, LR 1067±295, p=0.0001), which was attenuated by treatment with either MSCs (765±258, p=0.04 vs. LR) or MSC EVs (715±200, p=0.01 vs. LR). Similarly, in the lung, vascular permeability increased after HS/T in LR-treated mice (Sham 297±155, LR 791±331, p=0.001) and was also attenuated by treatment with MSCs (331±172, p=0.001 vs. LR) or MSC EVs (303±88, p=0.0004 vs. LR). The fluorescence intensities among mice treated with MSCs or MSC EVs were not significantly different from each other in either the small intestine (p=0.97) or the lung (p=0.99).

MSCs and MSC EVs decrease histopathologic injury in the small intestine and lung induced by HS/T

Histopathological analysis of the lungs revealed that HS/T mice treated with LR have significantly higher levels of inflammatory cell infiltrates compared to sham mice (p=0.004). Treatment with MSCs significantly attenuated the levels of inflammatory cell infiltrates (p=0.01 vs. LR), and there was a trend toward lower inflammatory cell infiltrates among mice treated with MSC EVs (p=0.07 vs. LR). The mean percentage of images with alveolar wall thickening per animal was 39% among sham mice, 60% among LR-treated mice, 37% among MSC-treated mice, and 45% among MSC EV-treated mice (Figure 4A, 4C).

Sections of small intestine evaluated using the Chiu grading system(31) demonstrated mild ischemic injury among LR-treated HS/T mice compared to sham mice (1.72±1.19 vs 0.19±0.31, p=0.005). Compared to LR-treated mice, MSC-treated mice had a mean score of 0.74±0.76 (p=0.06) and MSC EV-treated mice had a mean score of 0.36±0.33 (p=0.007) (Figure 4B, 4D).

MSC conditioned media protects against oxidative stress-induced intestinal epithelial monolayer permeability

To evaluate whether MSCs or MSC EVs have effects on epithelial barrier integrity in the gut, Caco-2 human intestinal epithelial cell monolayers were subjected to H_2O_2 challenge and impedance tracings were analyzed at 4k Hz to assess paracellular permeability. Impedance tracings and area-under-the-curve (AUC) calculations from cells pre-treated with MSC control media, MSC conditioned media (MSC CM), or MSC EVs are shown in Figure 2. MSC CM, which contains the secreted products of MSCs, significantly attenuated H_2O_2-induced permeability compared to control media, which had not been exposed to

MSCs (AUC 3.85 vs 3.56, p<0.001). In contrast to MSC CM, MSC EVs did not exert protective effects against H_2O_2-induced permeability (AUC 3.72 vs 3.66, p=0.83) (Figure 5).

DISCUSSION

This study demonstrates that systemic infusion of either MSCs or MSC EVs decreases vascular permeability and injury in the small intestine and lung in mice subjected to HS/T. Our data also demonstrate that MSC EVs infused early after HS/T traffic to multiple organs —predominantly to the liver and spleen but also to the lung and kidney within 30 minutes after delivery. Together these findings suggest that MSCs and MSC EVs may be able to mediate systemic therapeutic effects and attenuate multi-organ dysfunction in HS/T.

The gut is believed to be an important driver of systemic inflammation and MODS in critical illness, however therapies to protect intestinal integrity in these patients are limited.(8, 9, 35) In the present study both MSCs and MSC EVs mitigated intestinal injury *in vivo*, however in Caco-2 intestinal epithelial cell monolayers *in vitro,* only MSC CM was protective against H_2O_2-induced permeability as measured by an ECIS impedance assay. The divergent effects of MSC EVs *in vitro* and *in vivo* are similar to previous findings in our lab in which we demonstrated that both MSCs and MSC EVs were protective against HS/T-induced lung permeability *in vivo,* however in human lung endothelial cells *in vitro*, MSC CM but not MSC EVs were protective against thrombin-induced permeability.(22) Additionally, labeled MSC EVs were identified in multiple organs but not in the sections of small intestine that were obtained 30 minutes after administration. Together, the discrepancy between the *in vitro* and *in vivo* findings and the lack of EVs in the small intestine suggest that the protective effects of MSC EVs on the intestine *in vivo* may rely on interaction of the EVs with other cell types such as circulating inflammatory cells, specifically macrophages and neutrophils, which were not present in the Caco-2 cell culture. For example, others have found that MSC EVs exert protective effects on the gut both *in vitro* and *in vivo* in mouse models of colitis via the promotion of M2 macrophage polarization.(36, 37) We hypothesize that one reason why the MSC CM was still protective of the intestinal epithelial barrier *in vitro* even in the absence of inflammatory cells is that MSC CM contains the entire MSC secretome, which includes not only EVs but also other RNAs, proteins (e.g. cytokines, chemokines, and growth factors), and lipids which are biologically active and may be responsible for this finding. We have in the past found similar effects with MSCs in a model of TBI. In our murine models of TBI, we found that MSCs present in small numbers in the brain (4 cells per tissue section out of the 1×10^6 injected intravenously), but the MSCs had potent biological effects on the brain on blood brain barrier permeability and vascular protection.(38) We hypothesize that the effects of the MSC EVs are similar, i.e. the MSC EVs act systemically on both inflammation and vascular barrier protection. We are currently investigating further the effects of MSCs and MSC EVs on inflammation and gene expression to better elucidate the mechanism of benefit seen in this study on gut and lung injury after HS/T.

An important limitation of this study is that vascular permeability and injury were evaluated *in vivo* at a single time point after a single dose of MSCs or MSC EVs. We chose to evaluate these endpoints acutely 2 hours after resuscitation, a time point known to result in

vascular permeability and injury in the lung in mice subjected to HS/T. The rationale for early delivery of MSCs or MSC EVs after HS/T is to target the changes in inflammation and vascular barrier compromise that occur early after HS/T and likely are responsible for the development of MODS. However, the duration and longer-term effects of these therapies in HS/T are unknown and will require further investigation and may lend insight into the effects of these treatments on prolonged organ injury. It is possible that repeated dosing of MSCs or MSC EVs may provide longer lasting effects than a single dose shortly after injury occurs. A second limitation is that this model of HS/T involves controlled bleeding with complete hemostasis at the end of the shock period, which reduces variability in injury between mice but does not reflect hemorrhage in the typical trauma patient. Studies in models of uncontrolled hemorrhage are warranted. Third, the MSCs and MSC EVs were delivered intra-arterially in this model rather than intravenously. Although the intravenous route is more likely to be used clinically, both routes have been using in various preclinical models for systemic administration, and the MSC EV biodistribution in this study appears similar to other preclinical disease models where MSC EVs were administered intravenously.(39)

While the benefits of MSC- and EV-based therapies have been demonstrated in a variety of preclinical animal models involving organ injury and MODS, translating these therapies into patients in the trauma and critical care setting is only in its infancy.(12, 40) Fortunately, MSC-based therapy is a rapidly growing field with over 1,000 trials currently registered on clinicaltrials.gov and published completed trials showing positive results without serious adverse effects.(41) While others have expressed concern that MSC and MSC EVs have procoagulant effects *in vitro*,(42) a recent systematic review of randomized controlled trials found that intravascular MSC delivery does not increase the risk of thromboembolic complications in adults.(43) There are also a small but growing number of trials planned or currently underway evaluating EV-based therapies for diseases characterized by inflammation, including ARDS and COVID-19.(44) The present study suggests that MSCs and MSC EVs may also play a role in the treatment of patients after HS/T in order to mitigate MODS. Moreover, EV-based therapies offer several advantages over MSCs. As a cell-free therapy, EVs cannot proliferate and differentiate following administration, have a lower risk of vascular obstruction or capillary entrapment, and are stable in circulation.(45)

In conclusion, this study suggests that MSC EVs may be a potential cell-free therapy targeting multi-organ dysfunction in HS/T. MSC EVs trafficked to multiple organs and similar to MSCs were protective in both the small intestine and lungs in an acute model. MSC CM was also protective against intestinal epithelial permeability *in vitro*, however this finding was not seen with MSC EVs. Future investigation should further evaluate the mechanisms of action of MSCs and MSC EVs, timing of delivery after injury, and repeated dosing in order to optimize longer-term outcomes following HS/T and move toward translating these therapies into clinical trials.

Supplementary Material

Refer to Web version on PubMed Central for supplementary material.

Sources of Funding:

Mark Barry received funding from the National Health Lung and Blood Institute under Award Number R38HL143581. The contents of this research are solely the responsibility of the authors and do not necessarily represent the official views of the NIH. Funding for these studies was provided by UCSF intramural funds to Shibani Pati.

References

1. Sauaia A, Moore EE, Johnson JL, Chin TL, Banerjee A, Sperry JL, Maier RV, Burlew CC. Temporal trends of postinjury multiple-organ failure: still resource intensive, morbid, and lethal. J Trauma Acute Care Surg. 2014;76(3):582–92, discussion 92–3. [PubMed: 24553523]
2. Dewar DC, Tarrant SM, King KL, Balogh ZJ. Changes in the epidemiology and prediction of multiple-organ failure after injury. J Trauma Acute Care Surg. 2013;74(3):774–9. [PubMed: 23425734]
3. Ulvik A, Kvåle R, Wentzel-Larsen T, Flaatten H. Multiple organ failure after trauma affects even long-term survival and functional status. Crit Care. 2007;11(5):R95. [PubMed: 17784940]
4. Holcomb JB, Tilley BC, Baraniuk S, Fox EE, Wade CE, Podbielski JM, del Junco DJ, Brasel KJ, Bulger EM, Callcut RA, et al. Transfusion of plasma, platelets, and red blood cells in a 1:1:1 vs a 1:1:2 ratio and mortality in patients with severe trauma: the PROPPR randomized clinical trial. JAMA. 2015;313(5):471–82. [PubMed: 25647203]
5. Birkner DR, Halvachizadeh S, Pape HC, Pfeifer R. Mortality of Adult Respiratory Distress Syndrome in Trauma Patients: A Systematic Review over a Period of Four Decades. World J Surg. 2020;44(7):2243–54. [PubMed: 32179975]
6. Jenkins DH, Rappold JF, Badloe JF, Berséus O, Blackbourne L, Brohi KH, Butler FK, Cap AP, Cohen MJ, Davenport R, et al. Trauma hemostasis and oxygenation research position paper on remote damage control resuscitation: definitions, current practice, and knowledge gaps. Shock. 2014;41 Suppl 1:3–12.
7. Holcomb JB, Pati S. Optimal trauma resuscitation with plasma as the primary resuscitative fluid: the surgeon's perspective. Hematology Am Soc Hematol Educ Program. 2013;2013:656–9. [PubMed: 24319247]
8. Deitch EA, Xu D, Kaise VL. Role of the gut in the development of injury- and shock induced SIRS and MODS: the gut-lymph hypothesis, a review. Front Biosci. 2006;11:520–8. [PubMed: 16146750]
9. Altshuler AE, Kistler EB, Schmid-Schönbein GW. Autodigestion: Proteolytic Degradation and Multiple Organ Failure in Shock. Shock. 2016;45(5):483–9. [PubMed: 26717111]
10. Cotton BA, Reddy N, Hatch QM, LeFebvre E, Wade CE, Kozar RA, Gill BS, Albarado R, McNutt MK, Holcomb JB. Damage control resuscitation is associated with a reduction in resuscitation volumes and improvement in survival in 390 damage control laparotomy patients. Ann Surg. 2011;254(4):598–605. [PubMed: 21918426]
11. Langan NR, Eckert M, Martin MJ. Changing patterns of in-hospital deaths following implementation of damage control resuscitation practices in US forward military treatment facilities. JAMA Surg. 2014;149(9):904–12. [PubMed: 25029432]
12. Pati S, Pilia M, Grimsley JM, Karanikas AT, Oyeniyi B, Holcomb JB, Cap AP, Rasmussen TE. Cellular Therapies in Trauma and Critical Care Medicine: Forging New Frontiers. Shock. 2015;44(6):505–23. [PubMed: 26428845]
13. Huber-Lang M, Wiegner R, Lampl L, Brenner RE. Mesenchymal Stem Cells after Polytrauma: Actor and Target. Stem Cells Int. 2016;2016:6289825. [PubMed: 27340408]
14. Matthay MA, Pati S, Lee JW. Concise Review: Mesenchymal Stem (Stromal) Cells: Biology and Preclinical Evidence for Therapeutic Potential for Organ Dysfunction Following Trauma or Sepsis. Stem Cells. 2017;35(2):316–24. [PubMed: 27888550]
15. Pati S, Gerber MH, Menge TD, Wataha KA, Zhao Y, Baumgartner JA, Zhao J, Letourneau PA, Huby MP, Baer LA, et al. Bone marrow derived mesenchymal stem cells inhibit inflammation and preserve vascular endothelial integrity in the lungs after hemorrhagic shock. PLoS One. 2011;6(9):e25171. [PubMed: 21980392]

16. Jiang H, Qu L, Dou R, Lu L, Bian S, Zhu W. Potential role of mesenchymal stem cells in alleviating intestinal ischemia/reperfusion impairment. PLoS One. 2013;8(9):e74468. [PubMed: 24058571]
17. He XW, He XS, Lian L, Wu XJ, Lan P. Systemic infusion of bone marrow-derived mesenchymal stem cells for treatment of experimental colitis in mice. Dig Dis Sci. 2012;57(12):3136–44. [PubMed: 22752635]
18. Shen ZY, Zhang J, Song HL, Zheng WP. Bone-marrow mesenchymal stem cells reduce rat intestinal ischemia-reperfusion injury, ZO-1 downregulation and tight junction disruption via a TNF-α-regulated mechanism. World J Gastroenterol. 2013;19(23):3583–95. [PubMed: 23801859]
19. Doster DL, Jensen AR, Khaneki S, Markel TA. Mesenchymal stromal cell therapy for the treatment of intestinal ischemia: Defining the optimal cell isolate for maximum therapeutic benefit. Cytotherapy. 2016;18(12):1457–70. [PubMed: 27745788]
20. Baek G, Choi H, Kim Y, Lee HC, Choi C. Mesenchymal Stem Cell-Derived Extracellular Vesicles as Therapeutics and as a Drug Delivery Platform. Stem Cells Transl Med. 2019;8(9):880–6. [PubMed: 31045328]
21. Rani S, Ryan AE, Griffin MD, Ritter T. Mesenchymal Stem Cell-derived Extracellular Vesicles: Toward Cell-free Therapeutic Applications. Mol Ther. 2015;23(5):812–23. [PubMed: 25868399]
22. Potter DR, Miyazawa BY, Gibb SL, Deng X, Togaratti PP, Croze RH, Srivastava AK, Trivedi A, Matthay M, Holcomb JB, et al. Mesenchymal stem cell-derived extracellular vesicles attenuate pulmonary vascular permeability and lung injury induced by hemorrhagic shock and trauma. J Trauma Acute Care Surg. 2018;84(2):245–56. [PubMed: 29251710]
23. Monsel A, Zhu YG, Gennai S, Hao Q, Hu S, Rouby JJ, Rosenzwajg M, Matthay MA, Lee JW. Therapeutic Effects of Human Mesenchymal Stem Cell-derived Microvesicles in Severe Pneumonia in Mice. Am J Respir Crit Care Med. 2015;192(3):324–36. [PubMed: 26067592]
24. Liu J, Chen T, Lei P, Tang X, Huang P. Exosomes Released by Bone Marrow Mesenchymal Stem Cells Attenuate Lung Injury Induced by Intestinal Ischemia Reperfusion via the TLR4/NF-κB Pathway. Int J Med Sci. 2019;16(9):1238–44. [PubMed: 31588189]
25. Barry M, Trivedi A, Miyazawa BY, Vivona LR, Khakoo M, Zhang H, Pathipati P, Bagri A, Gatmaitan MG, Kozar R, et al. Cryoprecipitate Attenuates the Endotheliopathy of Trauma in Mice Subjected to Hemorrhagic Shock and Trauma. J Trauma Acute Care Surg. 2021.
26. Pati S, Potter DR, Baimukanova G, Farrel DH, Holcomb JB, Schreiber MA. Modulating the endotheliopathy of trauma: Factor concentrate versus fresh frozen plasma. J Trauma Acute Care Surg. 2016;80(4):576–84; discussion 84–5. [PubMed: 26808040]
27. Pati S, Peng Z, Wataha K, Miyazawa B, Potter DR, Kozar RA. Lyophilized plasma attenuates vascular permeability, inflammation and lung injury in hemorrhagic shock. PLoS One. 2018;13(2):e0192363. [PubMed: 29394283]
28. Lee C, Mitsialis SA, Aslam M, Vitali SH, Vergadi E, Konstantinou G, Sdrimas K, Fernandez-Gonzalez A, Kourembanas S. Exosomes mediate the cytoprotective action of mesenchymal stromal cells on hypoxia-induced pulmonary hypertension. Circulation. 2012;126(22):2601–11. [PubMed: 23114789]
29. Gatti S, Bruno S, Deregibus MC, Sordi A, Cantaluppi V, Tetta C, Camussi G. Microvesicles derived from human adult mesenchymal stem cells protect against ischaemia-reperfusion-induced acute and chronic kidney injury. Nephrol Dial Transplant. 2011;26(5):1474–83. [PubMed: 21324974]
30. Potter DR, Baimukanova G, Keating SM, Deng X, Chu JA, Gibb SL, Peng Z, Muench MO, Fomin ME, Spinella PC, et al. Fresh frozen plasma and spray-dried plasma mitigate pulmonary vascular permeability and inflammation in hemorrhagic shock. J Trauma Acute Care Surg. 2015;78(6 Suppl 1):S7–S17. [PubMed: 26002267]
31. Chiu CJ, McArdle AH, Brown R, Scott HJ, Gurd FN. Intestinal mucosal lesion in low-flow states. I. A morphological, hemodynamic, and metabolic reappraisal. Arch Surg. 1970;101(4):478–83. [PubMed: 5457245]
32. Théry C, Witwer KW, Aikawa E, Alcaraz MJ, Anderson JD, Andriantsitohaina R, Antoniou A, Arab T, Archer F, Atkin-Smith GK, et al. Minimal information for studies of extracellular vesicles 2018 (MISEV2018): a position statement of the International Society for Extracellular Vesicles

and update of the MISEV2014 guidelines. J Extracell Vesicles. 2018;7(1):1535750. [PubMed: 30637094]

33. Anderson P, Carrillo-Gálvez AB, García-Pérez A, Cobo M, Martín F. CD105 (endoglin)-negative murine mesenchymal stromal cells define a new multipotent subpopulation with distinct differentiation and immunomodulatory capacities. PLoS One. 2013;8(10):e76979. [PubMed: 24124603]
34. Wang D, Liu N, Xie Y, Song B, Kong S, Sun X. Different culture method changing CD105 expression in amniotic fluid MSCs without affecting differentiation ability or immune function. J Cell Mol Med. 2020;24(7):4212–22. [PubMed: 32119193]
35. Klingensmith NJ, Coopersmith CM. The Gut as the Motor of Multiple Organ Dysfunction in Critical Illness. Crit Care Clin. 2016;32(2):203–12. [PubMed: 27016162]
36. Cao L, Xu H, Wang G, Liu M, Tian D, Yuan Z. Extracellular vesicles derived from bone marrow mesenchymal stem cells attenuate dextran sodium sulfate-induced ulcerative colitis by promoting M2 macrophage polarization. Int Immunopharmacol. 2019;72:264–74. [PubMed: 31005036]
37. Song WJ, Li Q, Ryu MO, Ahn JO, Ha Bhang D, Chan Jung Y, Youn HY. TSG-6 Secreted by Human Adipose Tissue-derived Mesenchymal Stem Cells Ameliorates DSS-induced colitis by Inducing M2 Macrophage Polarization in Mice. Sci Rep. 2017;7(1):5187. [PubMed: 28701721]
38. Pati S, Khakoo AY, Zhao J, Jimenez F, Gerber MH, Harting M, Redell JB, Grill R, Matsuo Y, Guha S, et al. Human mesenchymal stem cells inhibit vascular permeability by modulating vascular endothelial cadherin/β-catenin signaling. Stem Cells Dev. 2011;20(1):89–101. [PubMed: 20446815]
39. Wen S, Dooner M, Papa E, Del Tatto M, Pereira M, Borgovan T, Cheng Y, Goldberg L, Liang O, Camussi G, et al. Biodistribution of Mesenchymal Stem Cell-Derived Extracellular Vesicles in a Radiation Injury Bone Marrow Murine Model. Int J Mol Sci. 2019;20(21).
40. Monsel A, Zhu YG, Gennai S, Hao Q, Liu J, Lee JW. Cell-based therapy for acute organ injury: preclinical evidence and ongoing clinical trials using mesenchymal stem cells. Anesthesiology. 2014;121(5):1099–121. [PubMed: 25211170]
41. Rodríguez-Fuentes DE, Fernández-Garza LE, Samia-Meza JA, Barrera-Barrera SA, Caplan AI, Barrera-Saldaña HA. Mesenchymal Stem Cells Current Clinical Applications: A Systematic Review. Arch Med Res. 2021;52(1):93–101. [PubMed: 32977984]
42. Silachev DN, Goryunov KV, Shpilyuk MA, Beznoschenko OS, Morozova NY, Kraevaya EE, Popkov VA, Pevzner IB, Zorova LD, Evtushenko EA, et al. Effect of MSCs and MSC-Derived Extracellular Vesicles on Human Blood Coagulation. Cells. 2019;8(3).
43. Thompson M, Mei SHJ, Wolfe D, Champagne J, Fergusson D, Stewart DJ, Sullivan KJ, Doxtator E, Lalu M, English SW, et al. Cell therapy with intravascular administration of mesenchymal stromal cells continues to appear safe: An updated systematic review and meta-analysis. EClinicalMedicine. 2020;19:100249. [PubMed: 31989101]
44. O'Driscoll L Extracellular vesicles from mesenchymal stem cells as a Covid-19 treatment. Drug Discov Today. 2020;25(7):1124–5. [PubMed: 32387262]
45. Parfejevs V, Sagini K, Buss A, Sobolevska K, Llorente A, Riekstina U, Abols A. Adult Stem Cell-Derived Extracellular Vesicles in Cancer Treatment: Opportunities and Challenges. Cells. 2020;9(5).

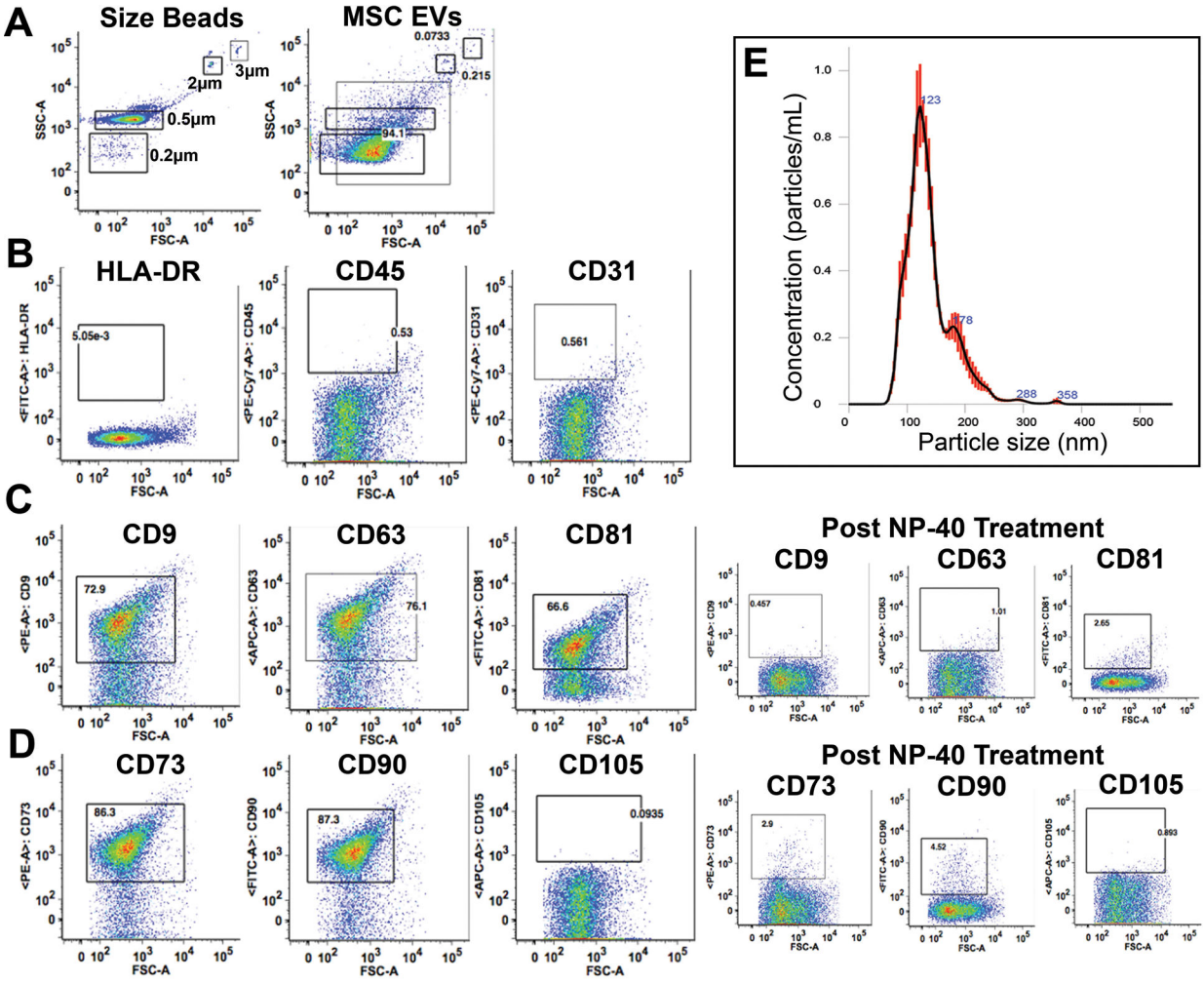

Figure 1. MSC EV characterization via flow cytometry and nanoparticle tracking analysis.

(A) EV size determination using size reference beads. (B) Negative markers for MSC EVs including HLA-DR, CD45, and CD31 were not expressed in the MSC EVs. (C) Positive expression of EV-specific markers CD9, CD63, and CD8. Treatment with NP-40 appropriately results in loss of expression of these markers. (D) Positive expression of MSC-origin specific markers CD73 and CD90 but not CD105. Treatment with NP-40 appropriately results in loss of expression of CD73 and CD90.

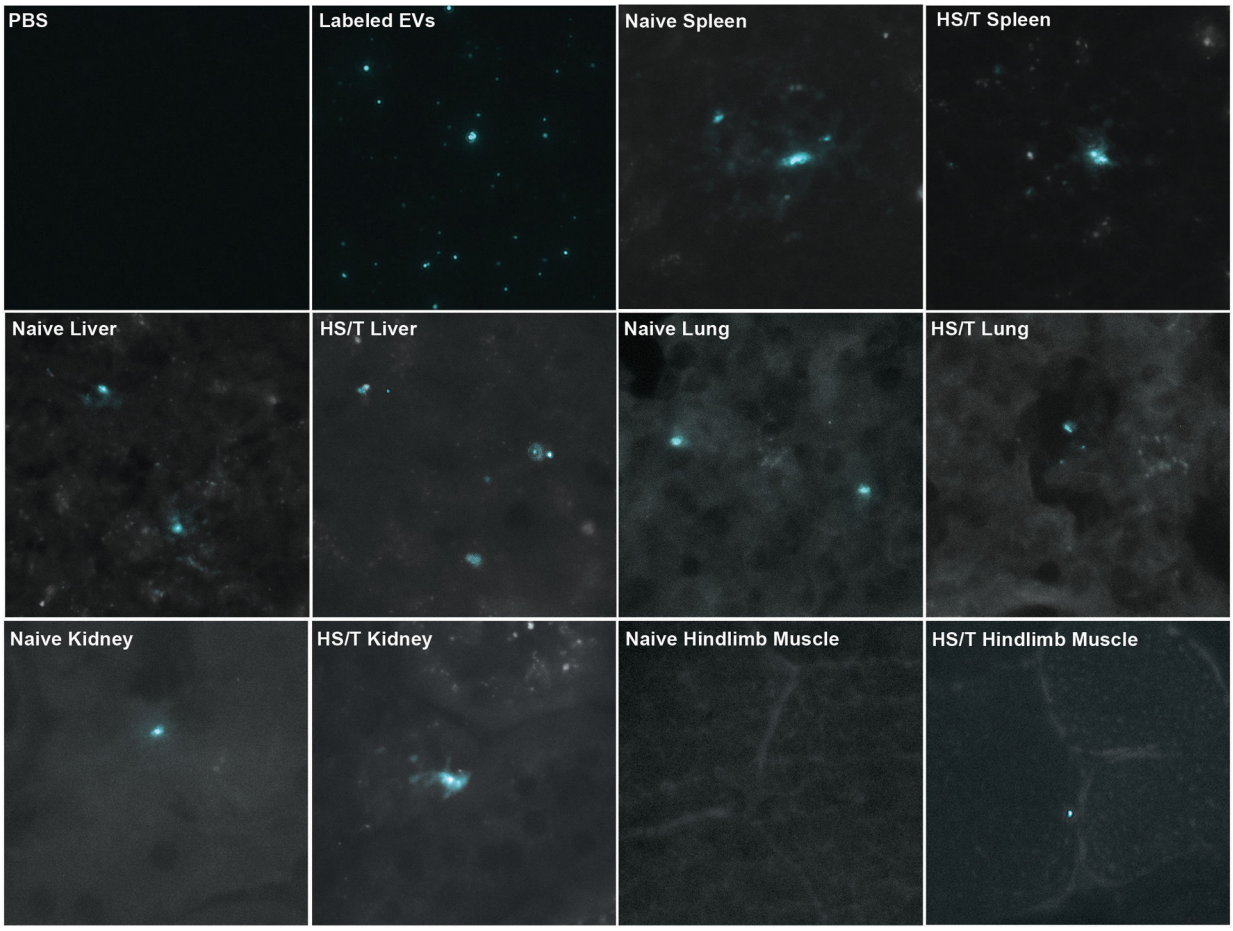

Figure 2. MSC EVs traffic to the liver, spleen, lungs, kidneys, and ischemic hindlimb muscle 30 minutes after delivery.

Far-red images are shown on the top left at 40x magnification of a slide with PBS and a slide with PBS containing labeled MSC EVs colorized cyan. The remaining images demonstrate presence of the labeled EVs predominantly in the liver and spleen but also in the lungs and kidneys of both the naïve mouse and the mouse subjected to HS/T. Labeled EVs were identified in the hindlimb muscle only in the mouse subjected to HS/T, which includes cannulation and subsequent ligation of the femoral artery. Labeled EVs were not detected in the blood or the small intestine at this time point.

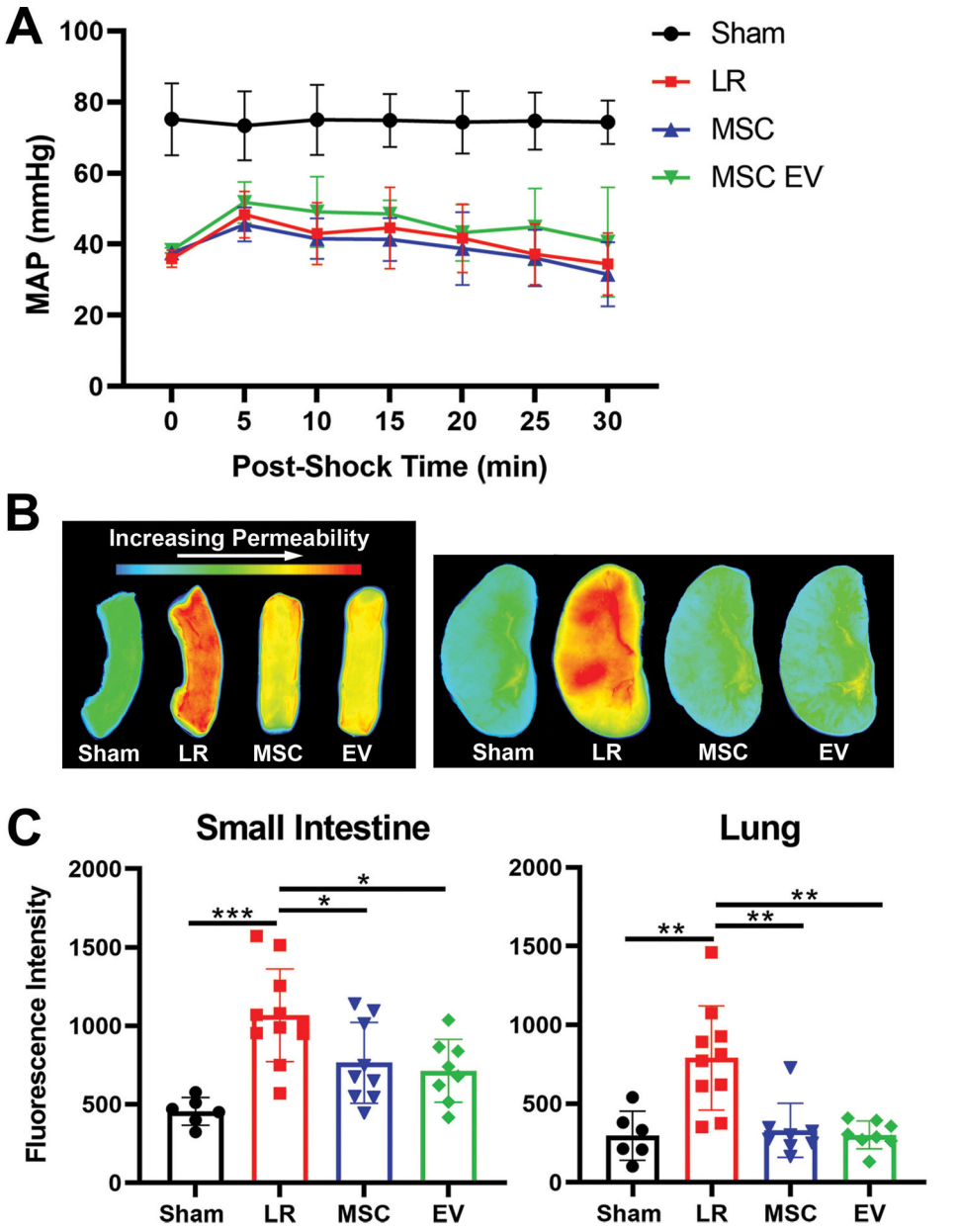

Figure 3. MSCs and MSC EVs are protective against vascular permeability in the small intestine and lungs *in vivo* in a mouse model of HS/T.

(A) Mean arterial pressures (MAPs) in mice subjected to HS/T are shown during the 30 minutes following resuscitation with LR, MSCs, or MSC EVs. MAPs were similar among LR-, MSC-, and MSC EV-treated animals. (B) Representative images of fluorescence intensity of dextran dye in the small intestine and lungs as a measure of vascular permeability. (C) Quantitation of fluorescence intensity demonstrating increased vascular permeability in the small intestine and lungs of LR-treated animals that was significantly reduced by treatment with either MSCs or MSC EVs. Columns indicate mean±SD. *p<0.05, **p<0.01, ***p<0.001 by one-way ANOVA with post-hoc Tukey's tests. N=6–10 mice per group.

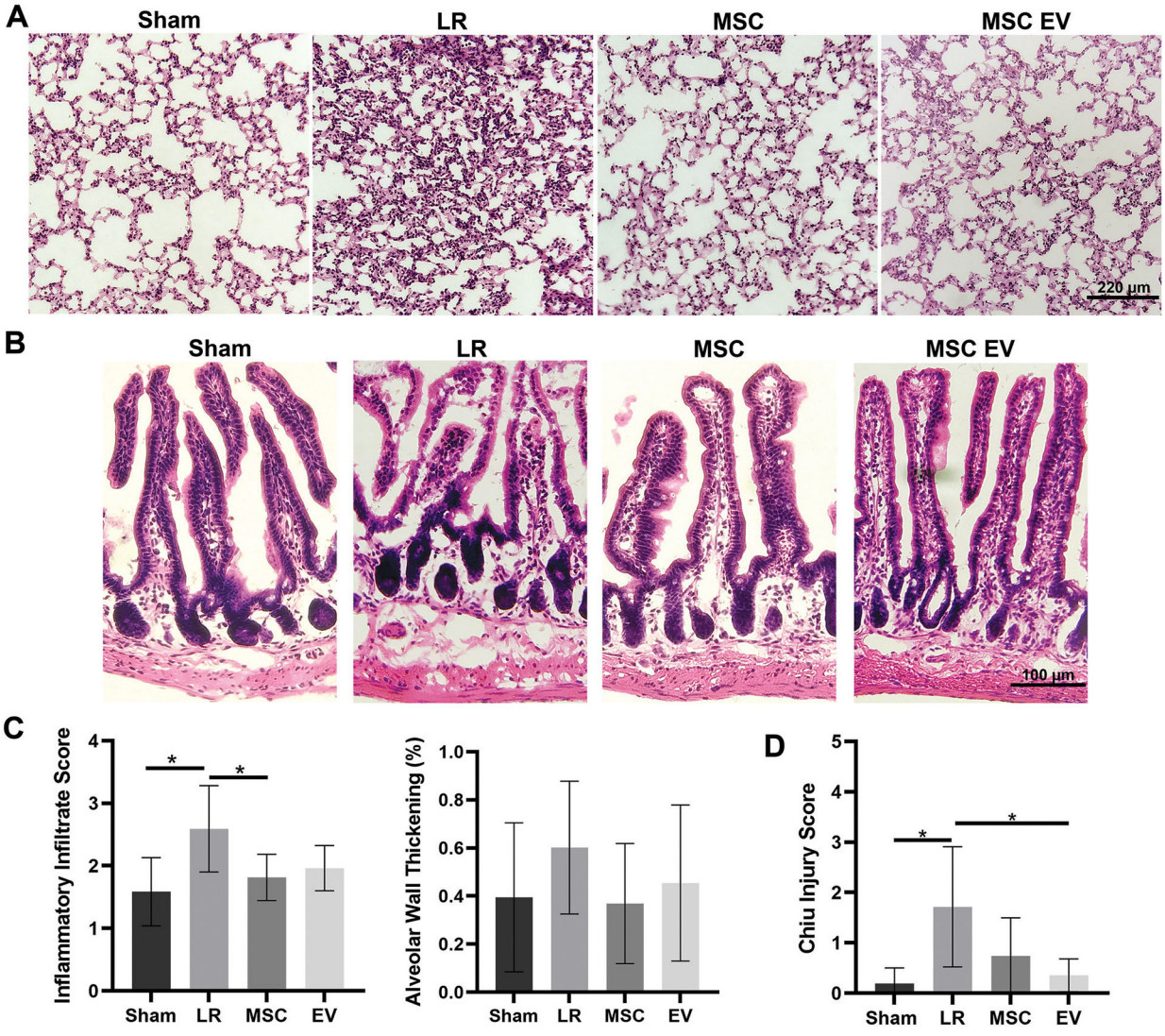

Figure 4. Histopathologic analysis of the small intestine and lungs after H&E stain.

(A) Representative images of the lungs and (B) representative images of the small intestine from each treatment group. (C) Quantitation of inflammatory infiltrates and presence of alveolar wall thickening in the lungs. The lungs of LR-treated mice had significantly increased inflammatory infiltrates compared to sham mice (p=0.004); MSC treatment significantly attenuated inflammatory cell infiltration compared to LR (p=0.01) and there was a trend toward attenuation by MSC EV treatment (p=0.07). Alveolar wall thickening scores were not significantly different between groups. (D) Mean Chiu ischemic injury score in the small intestine demonstrating significant injury in LR-treated mice compared to sham mice. Injury scores trended lower among MSC-treated mice compared to LR-treated mice (p=0.06) and were significantly lower among MSC EV-treated mice (p=0.007). *p<0.05 by one-way ANOVA with post-hoc Tukey's tests.

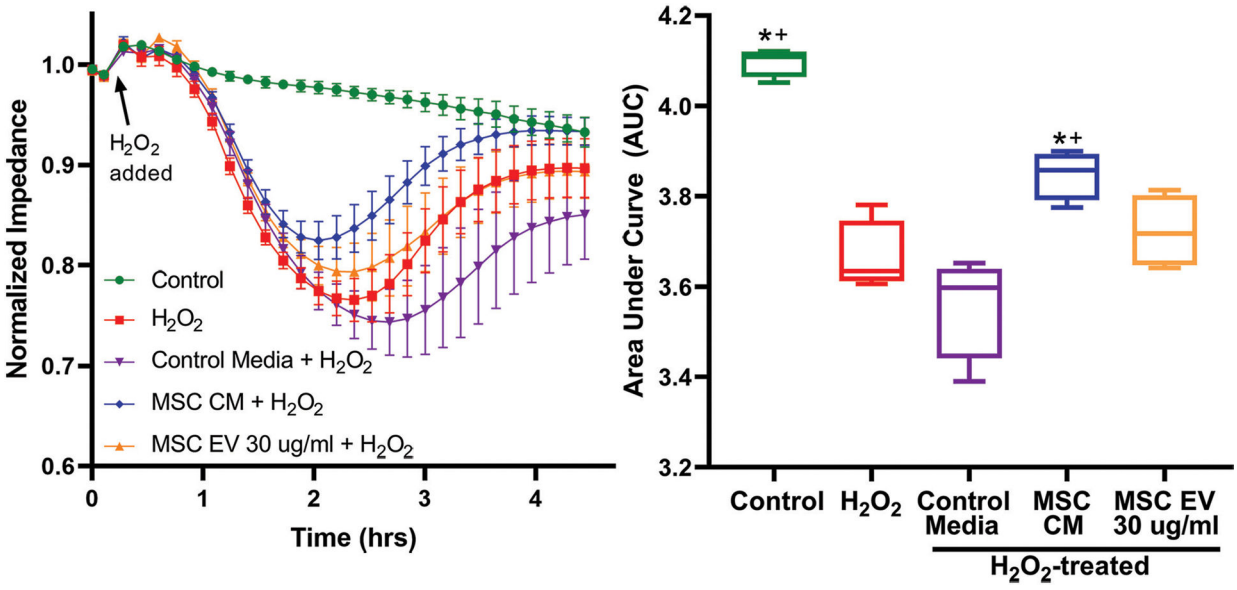

Figure 5. MSC CM and MSC EVs have differential effects *in vitro* in Caco-2 intestinal epithelial cell monolayers.

(A) ECIS impedance tracings after pre-treatment with MSC control media which has not been exposed to MSCs, MSC CM which contains the MSC secretome, or MSC EVs. (B) Area under the curve (AUC) quantitation after exposure to H_2O_2. *Indicates significant difference compared to control; + indicates significant difference compared to MSC control media by one-way ANOVA with post-hoc Tukey's tests ($p<0.05$). N=4 cell replicates per group.